HHS Public Access

Author manuscript

*Circ Genom Precis Med*. Author manuscript; available in PMC 2022 December 01.

Published in final edited form as:

*Circ Genom Precis Med*. 2021 December ; 14(6): e003419. doi:10.1161/CIRCGEN.121.003419.

# Mono- and Bi-allelic Protein Truncating Variants in Alpha-actinin 2 cause Cardiomyopathy through Distinct Mechanisms

**Malene E. Lindholm, PhD**[1,*], **David Jimenez-Morales, PhD**[1], **Han Zhu, MD**[1], **Kinya Seo, PhD**[1], **David Amar, PhD**[1], **Chunli Zhao, PhD**[1], **Archana Raja, MS**[1], **Roshni Madhvani, PhD**[1], **Sarah Abramowitz, BS**[1], **Cedric Espenel, PhD**[4], **Shirley Sutton, MS**[1], **Colleen Caleshu, ScM**[1,6], **Gerald J. Berry, MD**[5], **Kara S. Motonaga, MD**[2,3], **Kyla Dunn, MS**[2,3], **Julia Platt, MS**[1,2], **Euan A. Ashley, FRCP, DPhil**[1,2], **Matthew T. Wheeler, MD, PhD**[1,2,*]

[1.]Division of Cardiovascular Medicine, Department of Medicine, Stanford University School of Medicine, Stanford University, Stanford, USA.

[2.]Center for Inherited Cardiovascular Diseases, Stanford University School of Medicine, Stanford University, Stanford, USA

[3.]Division of Pediatric Cardiology, Department of Pediatrics, Stanford University School of Medicine, Stanford, USA

[4.]Cell Sciences Imaging Facility, Stanford University School of Medicine, Stanford, USA

[5.]Department of Pathology, Stanford University School of Medicine, Stanford, USA.

[6.]GeneMatters, San Francisco, CA

## Abstract

**Background:** Alpha-actinin 2 (ACTN2) anchors actin within cardiac sarcomeres. The mechanisms linking *ACTN2* mutations to myocardial disease phenotypes are unknown. Here, we characterize patients with novel *ACTN2* mutations to reveal insights into the physiological function of ACTN2.

**Methods:** Patients harboring ACTN2 protein-truncating variants were identified using a custom mutation pipeline. In patient-derived iPSC-cardiomyocytes, we investigated transcriptional profiles using RNA sequencing, contractile properties using video-based edge detection and cellular hypertrophy using immunohistochemistry. Structural changes were analyzed through electron microscopy. For mechanistic studies, we used co-immunoprecipitation for ACTN2, followed by

[*]Correspondence to: Matthew T Wheeler MD PhD, Stanford University School of Medicine, Division of Cardiovascular Medicine, FCRC, 870 Quarry Road, CV277, Stanford, CA 94305-5406, Ph: 650-725-5921, Fax: 650-725-1599, wheelerm@stanford.edu, Malene E Lindholm PhD, Stanford University School of Medicine, Division of Cardiovascular Medicine, FCRC, 870 Quarry Road, CV107, Stanford, CA 94305-5406, Ph: 650-725-5921, Fax: 650-725-1599, malenel@stanford.edu.

Author information

*Conceptualization:* M.E.L, E.A.A, M.T.W, *Methodology:* M.E.L, D.J-M, K.S, C.S, *Software:* D.J-M, D.A, A.R, *Formal analysis:* M.E.L, D.J-M, H.Z, K.S, D.A, C.E, *Investigation:* M.E.L, H.Z, K.S, R.M, S.A, S.S, C.C, K.S.M, K.D., J.P, M.T.W. *Resources:* G.J.B, *Writing - original draft:* M.E.L, *Writing - review and editing:* M.E.L, D.J-M, H.Z., E.A.A, M.T.W, *Visualization:* M.E.L, D.J-M., D.A., *Supervision:* E.A.A, M.T.W.

Disclosures

E.A.A. is founder at Personalis and DeepCell, Inc, and advisor for SequenceBio and Genome Medical. CC is an employee at GeneMatters. M.T.W. has ownership interest in Personalis. The other authors declare no competing interests.

mass-spectrometry to investigate protein-protein interaction, and protein tagging followed by confocal microscopy to investigate introduction of truncated ACTN2 into the sarcomeres.

**Results:** Patient-derived iPSC-cardiomyocytes were hypertrophic, displayed sarcomeric structural disarray, impaired contractility, and aberrant $Ca^{2+}$-signaling. In heterozygous indel cells, the truncated protein incorporates into cardiac sarcomeres, leading to aberrant Z-disc ultrastructure. In homozygous stop-gain cells, affinity-purification mass spectrometry reveals an intricate ACTN2 interactome with sarcomere and sarcolemma-associated proteins. Loss of the C-terminus of ACTN2 disrupts interaction with ACTN1 and GJA1, two sarcolemma-associated proteins, that may contribute to the clinical arrhythmic and relaxation defects. The causality of the stop-gain mutation was verified using CRISPR-Cas9 gene editing.

**Conclusions:** Together, these data advance our understanding of the role of ACTN2 in the human heart and establish recessive inheritance of *ACTN2* truncation as causative of disease.

### Keywords

Cardiomyopathy; Hypertrophy; Basic Science Research; Myocardial Biology; Contractile Function; Actinin cardiomyopathy; mass-spectrometry; cardiac contractility and energetics; hypertrophy

## Introduction

Inherited cardiomyopathy and arrhythmia syndromes are common indications for heart transplantation and leading causes of sudden cardiac death in children and adolescents. Clinical genetic testing of families with atypical presentations often leaves clinicians and families with variants of uncertain significance. Growing evidence has shown a diverse genetic etiology of early-onset cardiomyopathies including dilated, hypertrophic, restrictive, and arrhythmogenic cardiomyopathies due to mutations of genes of the sarcomere and the sarcolemma.[1,2]

Alpha-actinin 2 (*ACTN2*) is an integral sarcomeric protein known to cross-link sarcomeric actin and titin filaments in the Z-disc of cardiac- and skeletal-myocyte sarcomeres. It is primarily expressed in cardiac and skeletal muscle [3,4], where it forms an antiparallel homodimer, with an N-terminal actin-binding domain and a C-terminal titin-binding region containing a calmodulin-like and EF-hand (helix-loop-helix) domain.[5] Prior mechanistic work has shown multiple functions for ACTN2, including anchoring of proteins within the sarcomere [6–9], regulation of ion channels [10,11], and indirect control of striated muscle gene expression through enhanced transactivation activity of nuclear receptors.[12] A missense variant in *ACTN2* was first identified in a patient with dilated cardiomyopathy (DCM) in 2003.[13] Since then, additional studies have reported heterozygous missense variants in *ACTN2* that co-segregate with both dilated and hypertrophic cardiomyopathy (HCM).[14–18] Common genetic variation in a regulatory element modulating *ACTN2* expression was recently associated with heart failure with reduced ejection fraction.[19] Despite these association studies, there is limited evidence for *ACTN2* as a causative gene for cardiomyopathy.[20,21] In addition, very few studies have found truncating variants

in *ACTN2*, without evidence of clear genetic association [22–24], and the relationship of truncating variants with cardiac disease manifestations has not been established.

To date, only autosomal dominant inheritance of *ACTN2* variants has been described in association with striated muscle disease and there is very limited mechanistic data on how *ACTN2* mutations cause disease. Herein, we demonstrate how structurally aberrant ACTN2 causes cardiac disease through distinct mechanisms. We describe these genetic variations, resulting in truncated ACTN2 proteins, as causative of cardiomyopathy with prominent arrhythmic phenotypes in the heterozygous state, and as causative of a progressive, severe restrictive cardiomyopathy (RCM) when in the homozygous state. Moreover, our successful modeling of *ACTN2* genetic disease using hiPSC-CMs presents an opportunity to identify targeted therapies, which are especially pertinent for this young patient population.

## Methods

Detailed methods are available in the Supplemental material. All proteomic data have been made publicly available in the MassIVE repository (https://massive.ucsd.edu/ProteoSAFe/static/massive.jsp). Code for colocalization analysis are available here: https://github.com/bioimage-analysis/malene_colocalization. All other data associated with this study are available in the main text or the supplemental material. The study was approved by the institutional review board at Stanford University and informed consent was obtained from all human subjects for genetic testing and publication of findings. Patient-derived induced pluripotent stem cells were generated after human subject consent specifying stem cell generation, and with the approval of the Stanford Stem Cell Research Oversight panel. Isolation of NRVMs was approved by the Stanford Administrative Panel on Laboratory Animal Care (APLAC, protocol #22920).

## Results

### Protein-truncating variants in ACTN2 cause diverse cardiac symptoms

To explore if structural variation in ACTN2 is causative of early-onset cardiomyopathy, we identified patients in the Stanford Center for Inherited Cardiovascular Disease database with rare or novel *ACTN2* variants. The first patient showed homozygosity for a novel variant in *ACTN2,* p.Gln860Stop (Q860X), which is absent in gnomAD (https://gnomad.broadinstitute.org/). The patient presented in infancy with symptoms of tachypnea and reduced ejection fraction (pedigree presented in Fig. 1A). A diagnostic endomyocardial biopsy at age 16 showed non-specific hypertrophy and fine interstitial fibrosis, but no myofibrillar loss (Fig. 1G, Fig. I in the data supplement). The patient developed progressive heart failure symptoms and episodes of atrial fibrillation in her 20's, with an echocardiogram (ECG) notable for severe biatrial enlargement, moderate biventricular dysfunction, and diastolic dysfunction (Fig. 1F); right heart catheterization showed RCM with equalization of ventricular filling pressures. She underwent orthotopic heart transplantation at age 23. Explant ventricular myocardial tissue sections showed mild hypertrophy and severe interstitial fibrosis (Fig. 1G). To verify the sequence-identified *ACTN2* truncation and investigate possible nonsense-mediated decay, we isolated protein from the explanted left ventricle (LV), right ventricle (RV) and from a contemporaneous biopsy of intercostal

skeletal muscle. Protein levels of ACTN2 were normal in patient cardiac tissue compared to healthy control individuals, and data confirmed the sequence-based predicted size reduction of approximately 4kDa (Fig. 1H). We further characterized the patient's LV tissue through RNA sequencing (Fig. II, Dataset I). Gene set enrichment analysis (GSEA) showed enrichment of extracellular matrix remodeling, collagen biosynthesis, and mRNA splicing gene sets (Fig. II, Dataset II). Highly ranked genes included collagens (*e.g. COL1A1*, *COL1A2,* and *COL4A1*), fibronectin and transforming growth factor β, that have been shown to be involved in pathologic cardiomyocyte hypertrophy and fibrosis.[25] These findings were highly indicative of the observed fibrosis. Common markers of pathologic cardiomyocyte hypertrophy and cardiomyopathy, *e.g. NPPA* and *NPPB*, were also elevated. Although ACTN2 protein levels were similar in the patient and controls, ACTN2 transcription was higher in the patient (Fig. 1I, see Fig. III for qRT-PCR validation). To evaluate if ACTN2 is differentially expressed in DCM and heart failure, we compared ACTN2 expression levels in the LV of 25 healthy individuals, 24 DCM patients, and 21 patients with ischemic heart disease from the MAGNet consortium.[26] No difference in ACTN2 expression was observed in these samples (Fig. IV).

The second proband (Del 1) presented at age 16 with an episode of exertional syncope (individual IV-3 in Fig. 1B). ECG showed T-wave inversion and repolarization abnormalities (Fig. 1C). Clinical panel genetic testing identified a heterozygous, novel 4.3kb deletion in *ACTN2* of exons 8 through 10, (NC_000001.10:g.236898807_236903093del) classified as a variant of unknown significance. A comprehensive family history revealed diverse cardiac symptoms, including two early sudden cardiac deaths, ventricular tachyarrhythmias, atrial fibrillation, LV noncompaction and symptomatic heart failure. Subsequent clinical screening and single locus testing of 1$^{st}$ degree relatives of affected individuals identified six additional family members with manifestations of ventricular conduction delay on ECG, atrial arrhythmia, LV noncompaction cardiomyopathy, and/or symptoms consistent with early onset heart failure (Table I in the data supplement), each of whom harbored the *ACTN2* variant. Samples were also contributed by the proband's father, who exhibited extensive T-wave inversions on ECG, atrial fibrillation, and nonsustained ventricular tachycardia (Del 2, individual III-2 in Fig. 1B). The deletion in Family 2 was verified using Sanger sequencing, which, in addition to the deletion, identified a 41bp intronic insertion from a central region of intron 10 of ACTN2 (Fig. 1D). The resulting in-frame indel would translate into an internally truncated protein of 771 amino acids compared to the full-length ACTN2 of 894. The deleted region is shown in purple in the structural model of ACTN2, displayed as a dimer (Fig. 1E).

Genetic variants in *ACTN2* are rare and the gene is intolerant to loss of function variation (pLI score of 1.0). The number of unique exonic variants in GnomAD was 506 after removal of synonymous variants (search: Nov 12 2020). The distribution of variants per exon is illustrated in Fig. V in the data supplement. ClinVar (https://www.ncbi.nlm.nih.gov/clinvar/) reports 14 pathogenic and likely pathogenic variants within *ACTN2* (search: Mar 24 2021): 8 missense, 1 splice acceptor and 3 nonsense variants, including the variant belonging to the first patient included in this study, in addition to 390 clinical lab-reported variants of uncertain significance.

## Patient-derived hiPSC-cardiomyocytes display elevated expression of metabolic genes

To functionally model the disease caused by truncated ACTN2 proteins, we utilized patient-derived and healthy hiPSCs differentiated into cardiomyocytes (hiPSC-CMs). Pluripotency of the hiPSC lines was confirmed through immunofluorescence staining of four pluripotency-markers, and markers for the three germ layers following embryoid body formation of all patient hiPSC lines and the main healthy control line (Fig. VI). Presence of the *ACTN2* variants was confirmed through Sanger sequencing (Fig. 1D and Fig. VII in the data supplement). We also investigated two *ACTN2* enhancer variants recently associated with heart failure [19], and all hiPSC lines carried the reference variant (Fig. VII). Genomic integrity was further verified through karyotyping of two of the control lines and the Q860X line (data not shown). We started by performing RNA sequencing on the three patient hiPSC-CMs and two different control hiPSC-CMs. Basic features of the analysis are shown in Fig. VIII in the data supplement, and the full datasets are available (Datasets III–IV). Expression of *ACTN2* was somewhat higher in both Q860X (logFC 0.8) and the heterozygous patients (logFC 1.14). Interestingly, in all patients, the most elevated gene was *MYL2* (Q860X: logFC 5.23, Del: logFC 4.90), coding for the key contractile protein Myosin light chain 2. We performed GSEA to investigate the general pathways affected in disease. The top five non-redundant pathways for positive and negative enrichment for each comparison are listed in Dataset V (see Datasets VI–VII for a full list of pathways). Multiple pathways were common between the two genetic conditions (Fig. VIII in the data supplement). Notably, induction of metabolic pathways was a common feature, with respiratory electron transport and gluconeogenesis represented among the top five enriched pathways. In Q860X, receptor-type tyrosine-protein phosphatases was the top down-regulated pathway. In the patients with the heterozygous indel, lower expression level was seen for many structural genes associated with extracellular matrix organization and collagen formation.

To verify that the pathology is not due to lower ACTN2 levels, protein expression was investigated using Western Blot. There was no evidence of proteolytic or ER mediated degradation of the aberrant protein due to Q860X; protein levels were similar to controls. Interestingly, we found that the exon 8–10 indel allele also produces a protein product (Fig. 2A–B), although at lower levels compared to the full length protein. RNA sequencing data similarly showed evidence of limited nonsense mediated decay of the truncated transcript with relative expression of 20% and 30% in Del 1 and 2 respectively, in relation to the full length transcript (Fig. IX in the data supplement).

## Truncated ACTN2 causes contractile dysfunction

Next, we assessed the functional implications of a truncated ACTN2 protein. We utilized video-based edge detection to measure the contractile function of single hiPSC-CMs. A significantly lower contractile velocity was found in all patient lines, with no difference in relaxation velocity (Fig. 2C–D). There was no difference in contraction frequency (Fig. 2E) or amplitude (Fig. 2F), which measures the degree of cellular shortening during each contraction. Representative traces from the contractility analysis are shown in Fig. 2G. To confirm that the C-terminal truncation (Q860X) is the causal disease variant, we used CRISPR-Cas9 to introduce the truncation into healthy hiPSCs to investigate if that would

recapitulate the disease phenotype. Two different guide RNAs were introduced together with the Cas9 to cut out the C-terminal region of both copies of *ACTN2*. Sequencing and gel-based size verification were used to confirm successful gene editing (see Supplemental methods and Fig. X in the data supplement for details). After differentiation into hiPSC-CMs, single-cell contractility analysis was performed for the CRISPR:ed control line that mirrored the disease line (cr_Q860X, where the C-terminal truncation has been introduced into a healthy hiPSC line) compared to the isogenic healthy control line. Although there was no significant reduction in contractile velocity, there was a similar trend ($p=0.058$) to what was observed for Q860X (Fig. 2C). The differences in relaxation velocity (Fig. 2D) and contraction amplitude (Fig. 2F) for cr_Q860X was also similar to Q860X.

Next, because cellular $Ca^{2+}$ handling is key for cardiomyocyte contractile function, we investigated if this was altered as a consequence of structurally aberrant ACTN2. We loaded live hiPSC-CMs with a ratiometric $Ca^{2+}$-binding fluorescent probe and $Ca^{2+}$ signals were evaluated using the IonOptix system. Interestingly, both patients with the heterozygous indel (Del 1 and Del 2) showed higher intracellular $Ca^{2+}$ signalling ($\Delta F/F$) compared to controls, while there was no effect in the patient with the homozygous truncation (Q860X) (Fig. 2H–J). This suggests that the contractile dysfunction is at the sarcomeric level for the heterozygous family, where elevated $Ca^{2+}$ signalling fails to compensate for the low contractility. There was no difference in baseline $Ca^{2+}$ levels (Fig. 2I).

## ACTN2 dysfunction induces cardiomyocyte hypertrophy

In response to the hypertrophic phenotype of the patients, we continued by analyzing cell size in the hiPSC-CMs. Single hiPSC-CMs were fixed and fluorescently co-labelled with an actin probe and ACTN2 as a cardiomyocyte-specific marker. After imaging, cell edges were traced and analyzed, all blinded to disease status. Images of patterned cells for each patient line and a healthy control line are shown in Fig. 3A, also demonstrating successful incorporation of ACTN2 in patient line sarcomeres. Patient cells were hypertrophic compared to healthy control cells (Fig. 3B), which was also observed for the CRISPR:ed line (cr_Q860X, Fig. XI in the data supplement). To further determine the impact of a disrupted ACTN2 function on development of a hypertrophic phenotype, we used a knock down approach in NRVMs, where cells treated with an siRNA against ACTN2 displayed marked hypertrophy compared to scramble control cells (Fig. XI).

## Heterozygous indel in ACTN2 causes sarcomeric structural disarray

The expression of the truncated protein in the heterozygous family lead us to investigate the sarcomeric structure of the cardiomyocytes. Transmission electron microscopy (TEM) of the patient hiPSC-CMs revealed severe structural disarray of the sarcomeres (Fig. 3C). The sarcomeres were somewhat elongated, the Z-discs were larger and the I-bands were thicker compared to healthy control hiPSC-CMs (Fig. 3D–F). The Z-discs also displayed a zigzag-like shape. Similar structural abnormalities have been observed in skeletal muscle of a patient heterozygous for a missense variant in exon 18 of *ACTN2*, that was associated with a severe myopathy.[27] The C-terminal truncation in *ACTN2* did not cause any clear structural abnormalities, only an increase in the Z-disc thickness was observed (Fig. 3E).

The large structural consequence of a heterozygous indel in *ACTN2* in combination with successful translation of the truncated transcript lead us to hypothesize that the pathogenic effect of the indel is due to incorporation of the truncated protein product into the Z-disc. To test this, we transfected a FLAG-tagged ACTN2 gene, carrying the indel, using a pCMV vector in healthy control hiPSC-CMs (Fig. III in the data supplement). Confocal imaging of hiPSC-CMs stained with an anti-FLAG antibody showed incorporation of the protein carrying the large indel into the sarcomeres (Fig. 3G, Fig. XII in the data supplement), suggesting a dominant negative effect of the *ACTN2* indel, in concordance with the family history.

## C-terminal truncation of ACTN2 disrupts interaction with ACTN1 and GJA1

The normal $Ca^{2+}$ signaling and sarcomere structure in Q860X hiPSC-CMs does not explain the pathogenic contractile dysfunction. Because the patient is homozygous for the C-terminal truncation, we hypothesized that lack of a C-terminal interaction may explain the pathogenic phenotype. To investigate the ACTN2 interactome, we performed co-immunoprecipitation (co-IP) using an ACTN2 monoclonal antibody that had been tested for immunoprecipitation and that was verified to bind to the truncated protein through Western blot. The purified protein complexes were subsequently subjected to LC-MS/MS (Liquid chromatography with tandem mass-spectrometry) (Fig. 4A). An IgG pulldown was used to control for nonspecific binding.

The interactome of ACTN2 has not been previously investigated in cardiomyocytes or using AP-MS, while multiple interactors have been identified through co-fractionation in cell lines [28] and yeast two-hybrid screens [29], and a few in specific low-throughput affinity-purification experiments in other cell types.[30,31] In human iPSC-CMs we found multiple novel interactors, mainly associated with the cell membrane. Several proteins involved in endocytosis through clathrin-coated pits were significantly pulled down in both healthy WT cells and patient Q860X cells (Fig. 4B, Datasets VIII–IX). This demonstrates that ACTN2 plays a role in the cardiac cell membrane, and has a much more intricate regulatory role than what is known to date. Membrane protein extraction with detergent and ultracentrifugation from hiPSC-CMs showed abundant ACTN2 levels in the membrane fraction (Fig. XIII in the data supplement). Other studies have demonstrated that ACTN2 is required for the proper membrane localization of a $Ca^{2+}$-activated $K^+$-channel [10], and have shown interactions with membrane-associated proteins, for example Kv1.5 channels [30] and $Na_v1.5$ channels [32]. While ACTN2 itself was significantly pulled down as expected, other large structural proteins or their interactors rarely reach significance in pulldown experiments due to the size and abundance of these proteins. Titin (TTN), Actin (ACTC1), Palladin (PALLD), Synaptopodin (SYNPO2) and Myozenin (MYOZ2) are all high abundance sarcomeric proteins that are known interactors of ACTN2 [9], but did not reach significance in this analysis. Intensity values from mass-spectrometry are not quantitative, but the relative differences between the ACTN2 pulldown and the IgG control indicated higher levels with ACTN2 pulldown (Fig. XIII, Dataset VIII).

Two proteins that interacted with ACTN2 in control hiPSC-CMs, GJA1 and ACTN1, were not identified in the pulldown of the C-terminal truncated ACTN2. GJA1, or Connexin 43,

is the main connexin protein in cardiac muscle. It is a gap junction protein important for cardiac electrical conduction. The subcellular location of Connexin 43 in the sarcolemma again suggests an important role for ACTN2 in the membrane. There is no previous evidence of an interaction between ACTN2 and GJA1. ACTN1 is a non-muscle alpha-actinin that is ubiquitously expressed. It has been shown to heterodimerize with the other non-muscle alpha-actinin ACTN4.[33] There are no previous affinity-purification experiments that have shown interaction between ACTN1 and ACTN2, previous interaction data are from high throughput screens. [28,29] RNA sequencing data showed similar expression levels of the majority of proteins identified in the interactome, including ACTN1 and GJA1, supporting that this is not an effect of differences in expression. Only *ITLN1* (Intelectin 1) showed expression differences (lower in Q860X, Fig. XIII in the data supplement).

To corroborate these findings, we repeated the co-IP followed by Western Blot for ACTN1 and GJA1. ACTN1 was identified only in the control hiPSC-CMs with no visible pulldown in Q860X (Fig. 4C), in concordance with the mass-spectrometry data. ACTN2 pulldown in the cr_Q860X showed similarly reduced interaction with the introduction of the C-terminal truncation (Fig. 4D). Interestingly, we observed a higher level of ACTN1 in the unbound fraction of Q860X and cr_Q860X. We therefore analyzed ACTN1 levels in the cardiac tissue of the patient, and found elevated levels in both the left and right ventricle (Fig. 4E), a potential compensatory response to the dysfunctional interaction with ACTN2. It could also be indicative of the observed pathophysiology, as elevated ACTN1 protein levels have been observed in myocardium from failing hearts.[34] Lack of interaction with ACTN2 was observed despite the elevated levels of ACTN1 in the patient. For GJA1, we were unable to confirm interaction through Co-IP followed by Western Blot. To further investigate the ACTN1-ACTN2 and GJA1-ACTN2 interactions, we used double-label immunofluorescence in hiPSC-CMs followed by confocal microscopy imaging. The results showed a significant colocalization of GJA1 and ACTN1 with ACTN2 (Fig. XIV in the data supplement). Thus, we have demonstrated several lines of evidence to support an interaction between ACTN2 and ACTN1, and ACTN2 and GJA1 in cardiomyocytes. No difference in the colocalization between either protein was observed between WT and Q860X in this analysis.

## Discussion

We show how protein-truncating variants in *ACTN2* cause cardiomyopathy with prominent arrhythmic phenotypes in the heterozygous state, and a progressive, severe restrictive cardiomyopathy in the homozygous state. Through deep cellular phenotyping and functional assays, we have demonstrated plausible mechanisms for how these truncating variants cause disease and verified the causal nature through gene editing. Furthermore, our results have defined a protein-protein interaction network for ACTN2 in human iPSC-derived cardiomyocytes, suggesting the importance of novel signaling pathways in the pathogenesis of *ACTN2*-mutation associated cardiomyopathies.

ACTN2 is a highly conserved integral protein within skeletal muscle and cardiac sarcomeres.[4] The high-resolution three-dimensional structure of ACTN2 was recently revealed.[5] In *Drosophila*, lack of *ACTN2* is lethal [35], and it is required for locomotion and proper assembly of Z-disc like dense bodies in *C. elegans*. [36] In a Zebrafish

model, knockdown of *ACTN2* causes severe cardiac, skeletal muscle and ocular defects. Skeletal muscle manifestations included disorganized fibers, muscle weakness and overall immobility. Cardiac expression of *ACTN2* was observed already in the first stage of cardiogenesis, in both atria and ventricles. Mutant fish developed enlarged, dilated hearts, and increased Z-disc thickness [37], similar to what was observed in our patients. Importantly, this pathogenic phenotype could not be rescued by *ACTN3*, despite high structural similarity between the two isoforms. In the patients described here, the lack of specific regions of ACTN2 similarly lead to cardiac disease and milder skeletal muscle manifestations.

The study of protein functional domains typically requires protein engineering. Here, we have utilized natural experiments to study the function of two domains in ACTN2. In the heterozygous state, we demonstrated the successful translation of transcripts from the allele carrying the large indel, and their incorporation into cardiomyocyte sarcomeres. The extent of the structural changes observed, with larger Z-discs, likely lead to altered contractile properties, where elevated $Ca^{2+}$ signaling is a way for the cell to compensate for the contractile dysfunction. This establishes that protein-truncating *ACTN2* variants can have dominant negative effects causative of cardiomyopathy and arrhythmia.

The majority of genetic variants in sarcomeric genes that have been demonstrated to cause cardiac disease have been heterozygous. Our data show how a biallelic variant in *ACTN2* causes disease through a recessive model. *ACTN2* has a pLi score of 1; a complete intolerance to loss of function variation. However, this study describes a woman homozygous for a loss-of-function mutation in *ACTN2*, which presents an extremely rare case of a human C-terminal knockout. This patient has allowed us to study not only the pathogenic effect of this mutation, but also the physiological function of *ACTN2* and how lack of the C-terminal region disrupts the physiological role of ACTN2 in cardiomyocytes. The patient developed early-onset RCM with progression to end stage heart failure. Genes that have been associated with a restrictive phenotype are also associated with HCM and DCM, and many described families have members with each cardiomyopathy subtype. Examples include *MYBPC3*, *TNNI3*, *TNNT2*, *ACTC* and *MYH7*. Only one previous study has associated a likely pathogenic variant in the heterozygous state (p.N175Y) in *ACTN2* with RCM.[38] Our study is the first to show evidence for genetic variation in *ACTN2* as a cause of RCM through a recessive mode of inheritance.

This study has several limitations. While we demonstrate a lack of interaction with GJA1 and ACTN1 for a C-terminal truncated ACTN2, we have not directly demonstrated the functional consequence of this, or that this is the direct cause of pathogenicity. The cellular dysfunction was confirmed when removing the C-terminal region of ACTN2 through gene editing, which demonstrates the causal nature of the variant, while the optimal confirmation would be to correct the homozygous mutation in the patient cells. Further, there was no gene correction performed for the heterozygous indel.

Understanding underlying genetic causes of cardiomyopathy has major implications for diagnosis and screening of unaffected family members, and establishing the mechanisms that underpin disease pathogenesis is critical for development of targeted therapies. Multiple genetic variants in sarcomeric genes are well-established to cause different forms

of cardiomyopathy, *e.g. MYH7*, *MYBPC3*, *TTN* and *LMNA*. There are several recent papers suggesting that only a core set of genes, not including *ACTN2*, are causative of cardiomyopathy.[21,39] However, there are a growing number of publications that have associated genetic variants in *ACTN2* with cardiomyopathy [14–18,40], as well as a regulatory element of *ACTN2* that was recently associated with heart failure.[19] We believe that the previous associations, in combination with the evidence presented here for how two protein-truncating variants, one dominant negative and one recessive, cause cardiac disease with variable pathological presentation supports inclusion of *ACTN2* as a disease-causing gene for cardiomyopathy in humans. Moreover, our successful modeling of *ACTN2* genetic disease using hiPSC-CMs presents an opportunity to identify more targeted therapies and test the potential alleviating effect of different drugs directly on myopathic cells.

## Supplementary Material

Refer to Web version on PubMed Central for supplementary material.

## Acknowledgements

We thank Dr. Alex Dainis for providing RNA from early differentiation of control hiPS cells, and Kratika Singhal and Ryan Lieb at the Vincent Coates Foundation Mass Spectrometry Laboratory, Stanford University Mass Spectrometry for acquiring the LC-MS/MS data.

### Funding Sources

This research was supported in part by; the Knut and Alice Wallenberg Foundation (M.E.L), R01HL105993 from the National Institutes of Health (E.A.A), and ARRA Award Number 1S10RR026780–01 from the National Center for Research Resources (NCRR). Its contents are solely the responsibility of the authors and do not necessarily represent the official views of the NCRR or the National Institutes of Health.

## Data availability

All proteomic data are available here: https://massive.ucsd.edu/ProteoSAFe/static/massive.jsp. Code for colocalization analysis are available here: https://github.com/bioimage-analysis/malene_colocalization All other data associated with this study are available in the main text or the supplement.

## Non-standard Abbreviations and Acronyms

| | |
|---|---|
| **hiPSC-CM** | human induced pluripotent stem cell-derived cardiomyocytes |
| **NRVM** | neonatal rat ventricular myocytes |
| **GSEA** | gene set enrichment analysis |
| **TEM** | transmission electron microscopy |
| **LC-MS/MS** | Liquid chromatography with tandem mass-spectrometry |
| **AP-MS** | affinity-purification mass-spectrometry |
| **Co-IP** | co-immunoprecipitation |
| **FPKM** | Fragments Per Kilobase of transcripts per Million mapped reads |

## References


1. Yotti R, Seidman CE, Seidman JG. Advances in the Genetic Basis and Pathogenesis of Sarcomere Cardiomyopathies. Annu Rev Genomics Hum Genet 2019;20:129–153. [PubMed: 30978303]
2. McKenna WJ, Judge DP. Epidemiology of the inherited cardiomyopathies. Nat Rev Cardiol 2020. 10.1038/s41569-020-0428-2.
3. Murphy ACH, Young PW. The actinin family of actin cross-linking proteins - a genetic perspective. Cell Biosci 2015;5:49. [PubMed: 26312134]
4. Beggs AH, Byers TJ, Knoll JH, Boyce FM, Bruns GA, Kunkel LM. Cloning and characterization of two human skeletal muscle alpha-actinin genes located on chromosomes 1 and 11. J Biol Chem 1992;267:9281–9288. [PubMed: 1339456]
5. Ribeiro E de A Jr, Pinotsis N, Ghisleni A, Salmazo A, Konarev PV, Kostan J, Sjöblom B, Schreiner C, Polyansky AA, Gkougkoulia EA, et al. The structure and regulation of human muscle α-actinin. Cell 2014;159:1447–1460. [PubMed: 25433700]
6. Eilertsen KJ, Kazmierski ST, Keller TC 3rd. Interaction of alpha-actinin with cellular titin. Eur J Cell Biol 1997;74:361–364. [PubMed: 9438132]
7. Salmikangas P, van der Ven PFM, Lalowski M, Taivainen A, Zhao F, Suila H, Schröder R, Lappalainen P, Fürst DO, Carpén O. Myotilin, the limb-girdle muscular dystrophy 1A (LGMD1A) protein, cross-links actin filaments and controls sarcomere assembly. Hum Mol Genet 2003;12:189–203. [PubMed: 12499399]
8. Bang ML, Mudry RE, McElhinny AS, Trombitás K, Geach AJ, Yamasaki R, Sorimachi H, Granzier H, Gregorio CC, Labeit S. Myopalladin, a novel 145-kilodalton sarcomeric protein with multiple roles in Z-disc and I-band protein assemblies. J Cell Biol 2001;153:413–427. [PubMed: 11309420]
9. Sjöblom B, Salmazo A, Djinović-Carugo K. α-Actinin structure and regulation. Cell Mol Life Sci 2008;65:2688. [PubMed: 18488141]
10. Lu L, Timofeyev V, Li N, Rafizadeh S, Singapuri A, Harris TR, Chiamvimonvat N. Alpha-actinin2 cytoskeletal protein is required for the functional membrane localization of a Ca2+-activated K+ channel (SK2 channel). Proc Natl Acad Sci U S A 2009;106:18402–18407. [PubMed: 19815520]
11. Cukovic D, Lu GW, Wible B, Steele DF, Fedida D. A discrete amino terminal domain of Kv1.5 and Kv1.4 potassium channels interacts with the spectrin repeats of alpha-actinin-2. FEBS Lett 2001;498:87–92. [PubMed: 11389904]
12. Huang SM, Huang CJ, Wang WM, Kang JC, Hsu WC. The enhancement of nuclear receptor transcriptional activation by a mouse actin-binding protein, alpha actinin 2. J Mol Endocrinol 2004;32:481–496. [PubMed: 15072553]
13. Mohapatra B, Jimenez S, Lin JH, Bowles KR, Coveler KJ, Marx JG, Chrisco MA, Murphy RT, Lurie PR, Schwartz RJ, et al. Mutations in the muscle LIM protein and alpha-actinin-2 genes in dilated cardiomyopathy and endocardial fibroelastosis. Mol Genet Metab 2003;80:207–215. [PubMed: 14567970]
14. Chiu C, Bagnall RD, Ingles J, Yeates L, Kennerson M, Donald JA, Jormakka M, Lind JM, Semsarian C. Mutations in alpha-actinin-2 cause hypertrophic cardiomyopathy: a genome-wide analysis. J Am Coll Cardiol 2010;55:1127–1135. [PubMed: 20022194]
15. Bagnall RD, Molloy LK, Kalman JM, Semsarian C. Exome sequencing identifies a mutation in the ACTN2 gene in a family with idiopathic ventricular fibrillation, left ventricular noncompaction, and sudden death. BMC Med Genet 2014;15:99. [PubMed: 25224718]
16. Girolami F, Iascone M, Tomberli B, Bardi S, Benelli M, Marseglia G, Pescucci C, Pezzoli L, Sana ME, Basso C, et al. Novel α-actinin 2 variant associated with familial hypertrophic cardiomyopathy and juvenile atrial arrhythmias: a massively parallel sequencing study. Circ Cardiovasc Genet 2014;7:741–750. [PubMed: 25173926]
17. Fan L-L, Huang H, Jin J-Y, Li J-J, Chen Y-Q, Xiang R. Whole-Exome Sequencing Identifies a Novel Mutation (p.L320R) of Alpha-Actinin 2 in a Chinese Family with Dilated Cardiomyopathy and Ventricular Tachycardia. Cytogenet Genome Res 2019;157:148–152. [PubMed: 30630173]
18. Good J-M, Fellmann F, Bhuiyan ZA, Rotman S, Pruvot E, Schläpfer J. ACTN2 variant associated with a cardiac phenotype suggestive of left-dominant arrhythmogenic cardiomyopathy. HeartRhythm Case Reports 2020;6:15–19. [PubMed: 31956495]

19. Arvanitis M, Tampakakis E, Zhang Y, Wang W, Auton A, 23andMe Research Team, Dutta D, Glavaris S, Keramati A, Chatterjee N, et al. Genome-wide association and multi-omic analyses reveal ACTN2 as a gene linked to heart failure. Nat Commun 2020;11:1122. [PubMed: 32111823]
20. Walsh R, Buchan R, Wilk A, John S, Felkin LE, Thomson KL, Chiaw TH, Loong CCW, Pua CJ, Raphael C, et al. Defining the genetic architecture of hypertrophic cardiomyopathy: re-evaluating the role of non-sarcomeric genes. Eur Heart J 2017;38:3461–3468. [PubMed: 28082330]
21. Walsh R, Mazzarotto F, Whiffin N, Buchan R, Midwinter W, Wilk A, Li N, Felkin L, Ingold N, Govind R, et al. Quantitative approaches to variant classification increase the yield and precision of genetic testing in Mendelian diseases: the case of hypertrophic cardiomyopathy. Genome Med 2019;11:5. [PubMed: 30696458]
22. Zimmerman RS, Cox S, Lakdawala NK, Cirino A, Mancini-DiNardo D, Clark E, Leon A, Duffy E, White E, Baxter S, et al. A novel custom resequencing array for dilated cardiomyopathy. Genet Med 2010;12:268–278. [PubMed: 20474083]
23. Al-Wakeel-Marquard N, Degener F, Herbst C, Kühnisch J, Dartsch J, Schmitt B, Kuehne T, Messroghli D, Berger F, Klaassen S. RIKADA Study Reveals Risk Factors in Pediatric Primary Cardiomyopathy. J Am Heart Assoc 2019;8:e012531. [PubMed: 31333075]
24. Neubauer J, Lecca MR, Russo G, Bartsch C, Medeiros-Domingo A, Berger W, Haas C. Post-mortem whole-exome analysis in a large sudden infant death syndrome cohort with a focus on cardiovascular and metabolic genetic diseases. Eur J Hum Genet 2017;25:404–409. [PubMed: 28074886]
25. Ichiro Manabe, Takayuki Shindo, Ryozo Nagai. Gene Expression in Fibroblasts and Fibrosis. Circ Res 2002;91:1103–1113. [PubMed: 12480810]
26. Liu Y, Morley M, Brandimarto J, Hannenhalli S, Hu Y, Ashley EA, Tang WHW, Moravec CS, Margulies KB, Cappola TP, et al. RNA-Seq identifies novel myocardial gene expression signatures of heart failure. Genomics 2015;105:83–89. [PubMed: 25528681]
27. Lornage X, Romero NB, Grosgogeat CA, Malfatti E, Donkervoort S, Marchetti MM, Neuhaus SB, Foley AR, Labasse C, Schneider R, et al. ACTN2 mutations cause “Multiple structured Core Disease” (MsCD). Acta Neuropathol 2019;137:501–519. [PubMed: 30701273]
28. Havugimana PC, Hart GT, Nepusz T, Yang H, Turinsky AL, Li Z, Wang PI, Boutz DR, Fong V, Phanse S, et al. A census of human soluble protein complexes. Cell 2012;150:1068–1081. [PubMed: 22939629]
29. Sahni N, Yi S, Taipale M, Fuxman Bass JI, Coulombe-Huntington J, Yang F, Peng J, Weile J, Karras GI, Wang Y, et al. Widespread macromolecular interaction perturbations in human genetic disorders. Cell 2015;161:647–660. [PubMed: 25910212]
30. Maruoka ND, Steele DF, Au BP, Dan P, Zhang X, Moore ED, Fedida D. alpha-actinin-2 couples to cardiac Kv1.5 channels, regulating current density and channel localization in HEK cells. FEBS Lett 2000;473:188–194. [PubMed: 10812072]
31. Eldstrom J, Choi WS, Steele DF, Fedida D. SAP97 increases Kv1. 5 currents through an indirect N-terminal mechanism. FEBS Lett 2003. Available at 10.1016/S0014-5793(03)00668-9.
32. Ziane R, Huang H, Moghadaszadeh B, Beggs AH, Levesque G, Chahine M. Cell membrane expression of cardiac sodium channel Na(v)1.5 is modulated by alpha-actinin-2 interaction. Biochemistry 2010;49:166–178. [PubMed: 19943616]
33. Foley KS, Young PW. The non-muscle functions of actinins: an update. Biochem J 2014;459:1–13. [PubMed: 24627985]
34. Hein S, Block T, Zimmermann R, Kostin S, Scheffold T, Kubin T, Klövekorn W-P, Schaper J. Deposition of nonsarcomeric alpha-actinin in cardiomyocytes from patients with dilated cardiomyopathy or chronic pressure overload. Exp Clin Cardiol 2009;14:e68–75. [PubMed: 20098571]
35. Fyrberg C, Ketchum A, Ball E, Fyrberg E. Characterization of lethal Drosophila melanogaster alpha-actinin mutants. Biochem Genet 1998;36:299–310. [PubMed: 9919356]
36. Moulder GL, Cremona GH, Duerr J, Stirman JN, Fields SD, Martin W, Qadota H, Benian GM, Lu H, Barstead RJ. α-actinin is required for the proper assembly of Z-disk/focal-adhesion-like structures and for efficient locomotion in Caenorhabditis elegans. J Mol Biol 2010;403:516–528. [PubMed: 20850453]

37. Yang J, Xu X. α-Actinin2 is required for the lateral alignment of Z discs and ventricular chamber enlargement during zebrafish cardiogenesis. FASEB J 2012;26:4230–4242. [PubMed: 22767232]
38. Kostareva A, Kiselev A, Gudkova A, Frishman G, Ruepp A, Frishman D, Smolina N, Tarnovskaya S, Nilsson D, Zlotina A, et al. Genetic Spectrum of Idiopathic Restrictive Cardiomyopathy Uncovered by Next-Generation Sequencing. PLoS One 2016;11:e0163362. [PubMed: 27662471]
39. Mazzarotto F, Tayal U, Buchan RJ, Midwinter W, Wilk A, Whiffin N, Govind R, Mazaika E, de Marvao A, Dawes TJW, et al. Reevaluating the Genetic Contribution of Monogenic Dilated Cardiomyopathy. Circulation 2020;141:387–398. [PubMed: 31983221]
40. Isbister JC, Nowak N, Butters A, Yeates L, Gray B, Sy RW, Ingles J, Bagnall RD, Semsarian C. "Concealed cardiomyopathy" as a cause of previously unexplained sudden cardiac arrest. Int J Cardiol 2021;324:96–101. [PubMed: 32931854]
41. Lek M, Karczewski KJ, Minikel EV, Samocha KE, Banks E, Fennell T, O'Donnell-Luria AH, Ware JS, Hill AJ, Cummings BB, et al. . Analysis of protein-coding genetic variation in 60,706 humans. Nature 2016;536:285–291. [PubMed: 27535533]
42. Zhao C, Farruggio AP, Bjornson CRR, Chavez CL, Geisinger JM, Neal TL, Karow M, Calos MP. Recombinase-mediated reprogramming and dystrophin gene addition in mdx mouse induced pluripotent stem cells. PLoS One 2014;9:e96279. [PubMed: 24781921]
43. Lian X, Zhang J, Azarin SM, Zhu K, Hazeltine LB, Bao X, Hsiao C, Kamp TJ, Palecek SP. Directed cardiomyocyte differentiation from human pluripotent stem cells by modulating Wnt/β-catenin signaling under fully defined conditions. Nat Protoc 2013;8:162–175. [PubMed: 23257984]
44. Ritchie ME, Phipson B, Wu D, Hu Y, Law CW, Shi W, Smyth GK. limma powers differential expression analyses for RNA-sequencing and microarray studies. Nucleic Acids Res 2015;43:e47. [PubMed: 25605792]
45. Subramanian A, Tamayo P, Mootha VK, Mukherjee S, Ebert BL, Gillette MA, Paulovich A, Pomeroy SL, Golub TR, Lander ES, et al. Gene set enrichment analysis: a knowledge-based approach for interpreting genome-wide expression profiles. Proc Natl Acad Sci U S A 2005;102:15545–15550. [PubMed: 16199517]
46. Ribeiro AJS, Ang Y-S, Fu J-D, Rivas RN, Mohamed TMA, Higgs GC, Srivastava D, Pruitt BL. Contractility of single cardiomyocytes differentiated from pluripotent stem cells depends on physiological shape and substrate stiffness. Proc Natl Acad Sci U S A 2015;112:12705–12710. [PubMed: 26417073]
47. Feaster TK, Cadar AG, Wang L, Williams CH, Chun YW, Hempel JE, Bloodworth N, Merryman WD, Lim CC, Wu JC, et al. Matrigel Mattress: A Method for the Generation of Single Contracting Human-Induced Pluripotent Stem Cell-Derived Cardiomyocytes. Circ Res 2015;117:995–1000. [PubMed: 26429802]
48. Pointon A, Harmer AR, Dale IL, Abi-Gerges N, Bowes J, Pollard C, Garside H. Assessment of cardiomyocyte contraction in human-induced pluripotent stem cell-derived cardiomyocytes. Toxicol Sci 2015;144:227–237. [PubMed: 25538221]
49. Hwang HS, Kryshtal DO, Feaster TK, Sánchez-Freire V, Zhang J, Kamp TJ, Hong CC, Wu JC, Knollmann BC. Comparable calcium handling of human iPSC-derived cardiomyocytes generated by multiple laboratories. J Mol Cell Cardiol 2015;85:79–88. [PubMed: 25982839]
50. UniProt Consortium T UniProt: the universal protein knowledgebase. Nucleic Acids Res 2018;46:2699. [PubMed: 29425356]
51. Jimenez-Morales D, RC A, Von Dollen J, Swaney D. artMS: Analytical R tools for Mass Spectrometry (R package version 1.6.5) 2020. Available at http://bioconductor.org/packages/release/bioc/html/artMS.html.
52. van der Walt S, Schönberger JL, Nunez-Iglesias J, Boulogne F, Warner JD, Yager N, Gouillart E, Yu T, scikit-image contributors. scikit-image: image processing in Python. PeerJ 2014;2:e453. [PubMed: 25024921]
53. van der Walt S, Colbert SC, Varoquaux G. The NumPy Array: A Structure for Efficient Numerical Computation. Computing in Science Engineering 2011;13:22–30.

54. Virtanen P, Gommers R, Oliphant TE, Haberland M, Reddy T, Cournapeau D, Burovski E, Peterson P, Weckesser W, Bright J, et al. SciPy 1.0: fundamental algorithms for scientific computing in Python. Nat Methods 2020;17:261–272. [PubMed: 32015543]

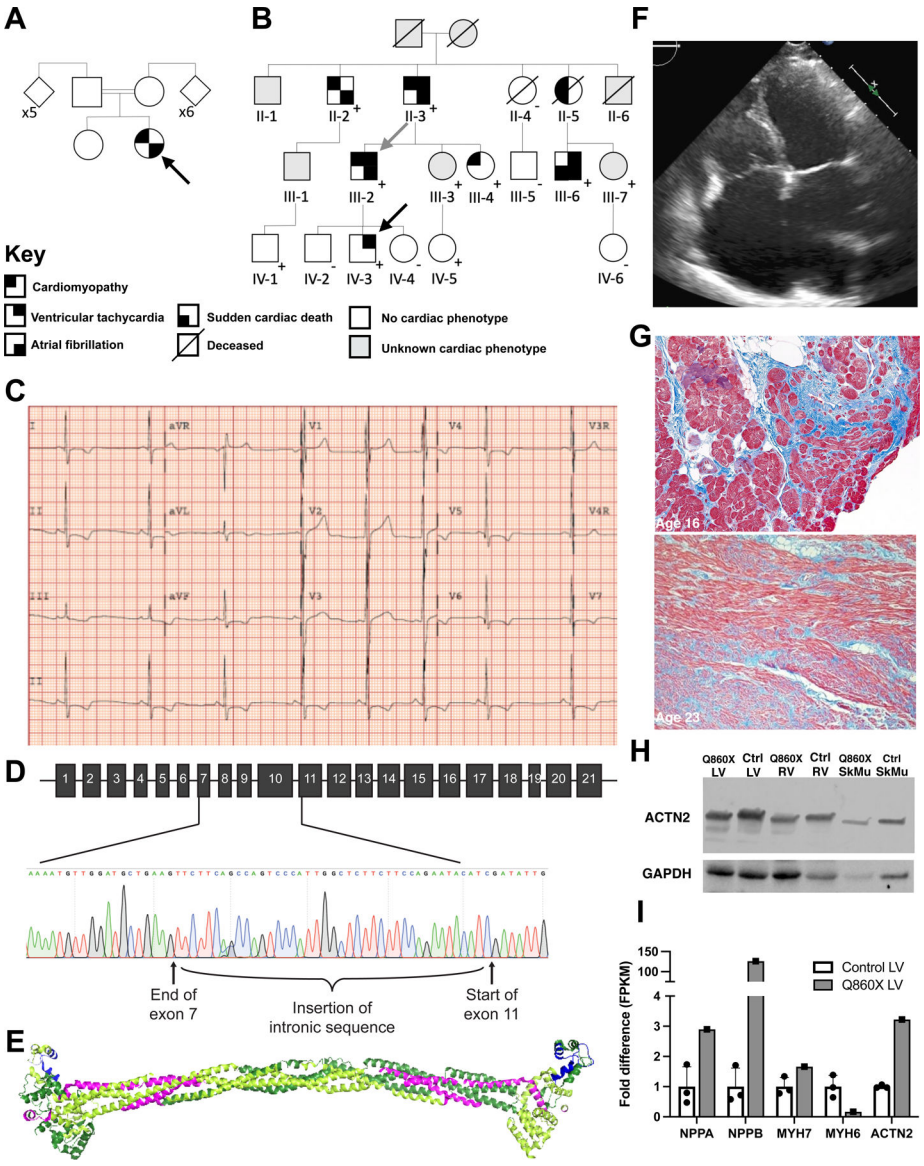


**Fig. 1. Protein-truncating alpha-actinin 2 variants cause diverse cardiac symptoms.**

A) Pedigree for a patient homozygous for a C-terminal truncation of ACTN2 (Q860X, proband indicated with an arrow). B) Pedigree for a family heterozygous for a large indel in ACTN2 (Del). Proband (Del 1) is indicated with a black arrow. Proband's father (Del 2), also carrying the mutation, is indicated with a grey arrow. Individuals with a + have confirmed ACTN2 deletion, while - indicates two full copies of ACTN2. Individuals with no sign have not been genetically tested. C) ECG recordings of Del 1 shows T-wave inversion. D) Sanger sequencing showed insertion of a 41bp intronic sequence in addition to the exon 8–10 deletion in the Del family, producing an inframe indel. E) The protein-level truncating variants shown in the 3D structure of ACTN2, displayed as the functional antiparallel dimer. The Q860X missing C-terminal region is shown in blue, and the exon 8–10 deletion in purple. F) Transthoracic echocardiography of Q860X showed restrictive cardiomyopathy. G) Trichrome staining of an endomyocardial biopsy obtained at age 16 (top) and the explanted

LV tissue from transplant at age 23 (bottom) showed coarse and fine interstitial fibrosis of cardiomyopathy. H) Western blot analysis of ACTN2 protein expression in the cardiac tissue indicated no nonsense-mediated decay, and confirmed the predicted size reduction of the protein by 4kDa. I) RNAseq analysis of the Q860X patient's left ventricle (LV, n=1) compared to healthy human control left ventricle tissue (n=3 individuals) showed elevated expression of known markers of hypertrophy (*NPPA* and *NPPB*), and of ACTN2 itself. Data is shown as fold difference (FD) in FPKM (Fragments Per Kilobase of transcripts per Million mapped reads). Bars show a normalized mean of 1 ± SEM for the 3 control hearts, and the individual FD value for Q860X. Z-scores for each gene when comparing Q860X with Ctrls: NPPA 1.49, NPPB 1.97, MYH7 1.50, MYH6 −1.88, ACTN2 1.99.

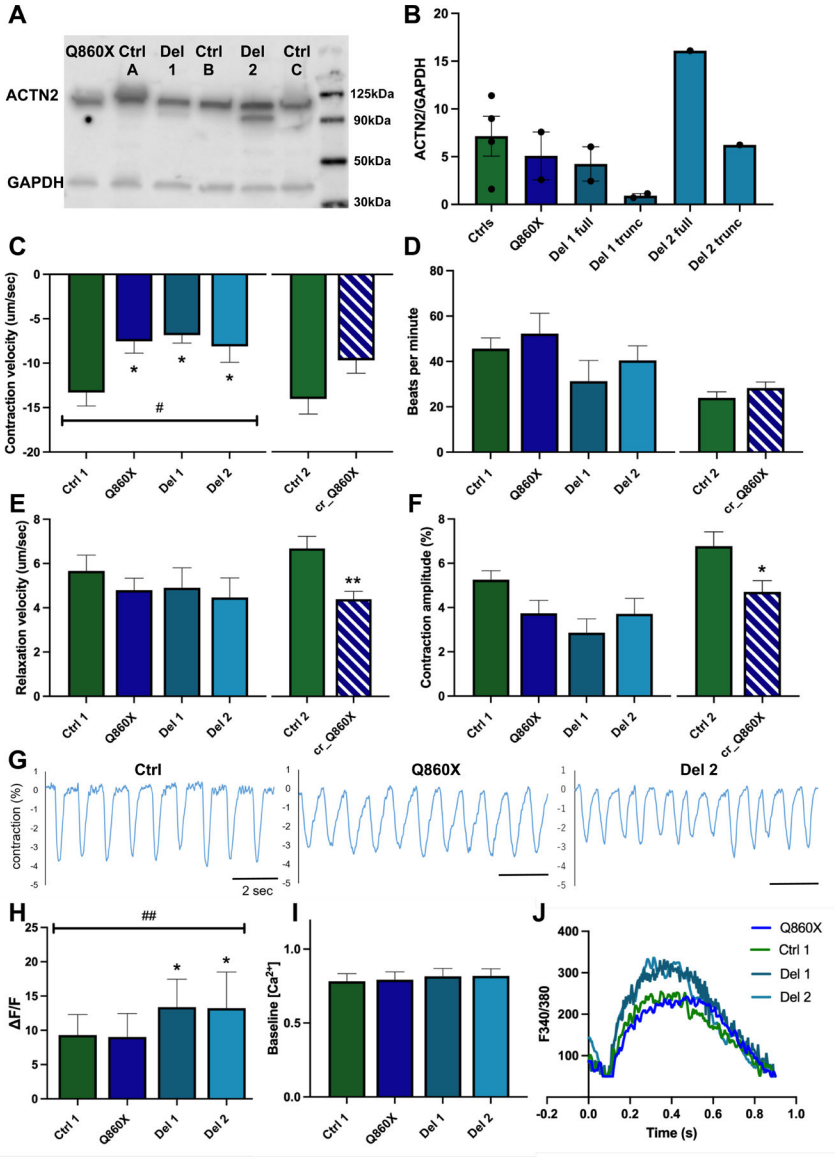


**Fig. 2. ACTN2 truncation causes contractile dysfunction.**

A-B) Western blot analysis showed that hiPSC-CMs from Q860X, Del 1 and Del 2 expressed ACTN2. Del 1 and Del 2 expressed both the full-length protein (full) and the truncated protein product (Del 1 trunc, Del 2 trunc), although at a lower level compared to the full length protein. N=4 control lines (Ctrls), N=2 different differentiation batches for Q860X and Del1 and N=1 batch for Del 2. C-F) Contractility analysis of spontaneously beating, single-cell hiPSC-CMs using video-based edge detection through the IonOptix system. (Ctrl 1 = control line A, N=12 cells, Q860X = patient with ACTN2 C-terminal truncation, N=12 cells, Del 1 = proband with heterozygous indel, N=6 cells, Del 2 = proband's father, also with heterozygous indel in ACTN2, N=12 cells, cr_Q860X = control line (A) with C-terminal section of ACTN2 removed, N=20 cells, Ctrl = isogenic control line (A) differentiated and run in the same batch as cr_Q860X, N=19 cells). G) Representative traces from the contractile analysis. H-J) $Ca^{2+}$-handling analysis of paced

single cell hiPSC-CMs (Ctrl A batch 1 N=17, Q860X N=19, Del 1 N=10, Del 2 N=14). Cells were loaded with a ratiometric $Ca^{2+}$ probe and analyzed using video-based edge detection through the IonOptix system. All cells were paced at 1Hz. ΔF/F is shown in (H) and baseline transient in (I). For contractility and $Ca^{2+}$-handling analysis, cells were cultured on 10 kPa micropatterns to get a more mature, elongated shape. Bars show mean ± SEM. * indicates significant difference compared to the control group at $P<0.05$ using a one-way ANOVA with Dunnett's multiple comparisons test. J) Average traces for all measured cells for each line, normalized by background subtraction.

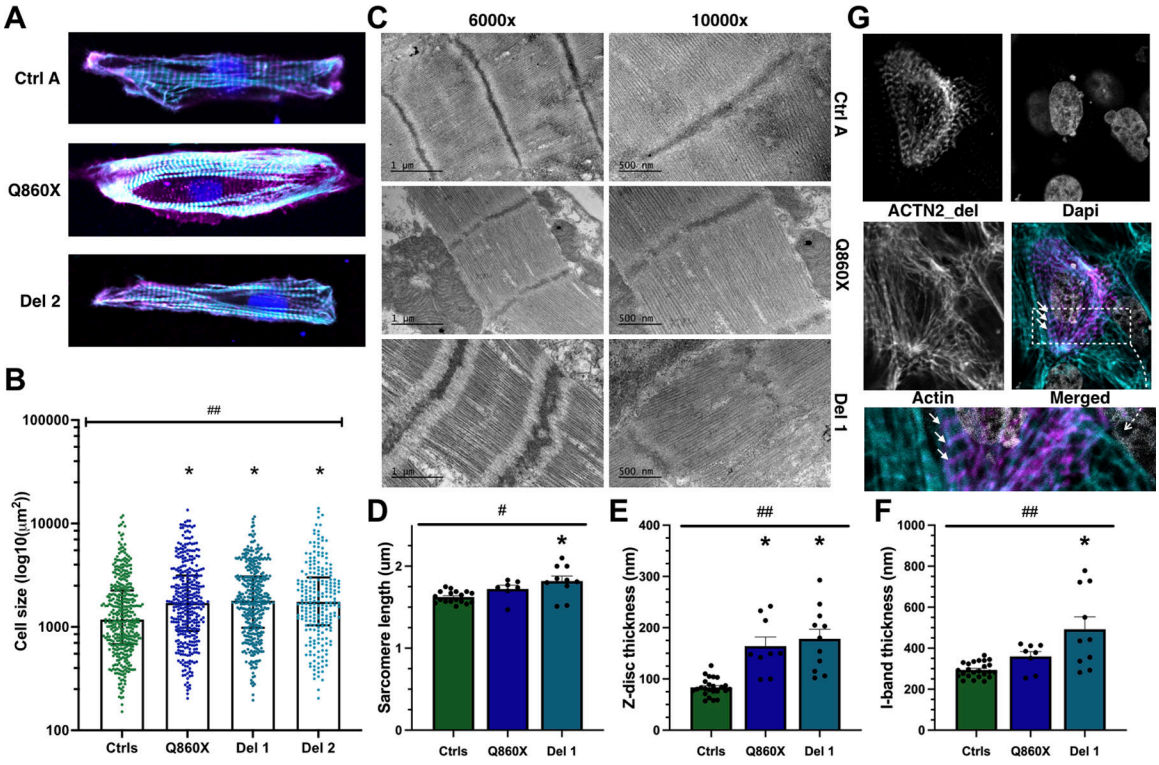


**Fig. 3. Patient-specific hiPSC-CMs are hypertrophic and display sarcomeric structural disarray.**

A) Representative hiPSC-CMs from each line cultured on 10 kPa micropatterns to get a more mature, elongated shape. ACTN2 is shown in purple, actin in turquoise and nuclei in blue (Dapi). B) Cell size of single-cell hiPSC-CMs. Ctrls represent hiPSC-CMs from 3 different healthy humans, N=399 individual cells total. Q860X N=356 cells, Del 1=379 cells and Del 2=226 cells. C) Representative transmission electron microscopy images of control hiPSC-CMs, Q860X and Del 1 at two different magnifications (6000X and 10000X). D-F) Quantitative analysis of the electron microscopy images. hiPSC-CMs from two different healthy humans were imaged for comparison with patient iPSC-CMs D) Sarcomere length (Ctrls N=18, Q860X N=7, Del 1 N=10). E) Z-disc thickness (Ctrls N=24, Q860X N=9, Del 1 N=11). F) I-band thickness (Ctrls N=24, Q860X N=8, Del 1 N=10). Bars show mean ± SEM. Significant effect from a one-way ANOVA analysis at $P<0.01$ is indicated by #, at $P<0.0001$ by ##. * indicates significant difference compared to control at $P<0.001$ using Dunnett's multiple comparisons test. G) Representative confocal image of cells transfected with a vector carrying a FLAG-tagged version of ACTN2_del. Image split into the FLAG-tagged ACTN2_del (top left), actin (lower left), Dapi for nuclei (top right), and a merged image with ACTN2_del shown in purple, actin in turquoise and nuclei in grey (lower right). A larger section highlighting the FLAG-tagged ACTN2 in purple is shown at the bottom. White arrows point to examples where the FLAG-tagged protein carrying the indel has been incorporated into the hiPSC-CM sarcomeres.

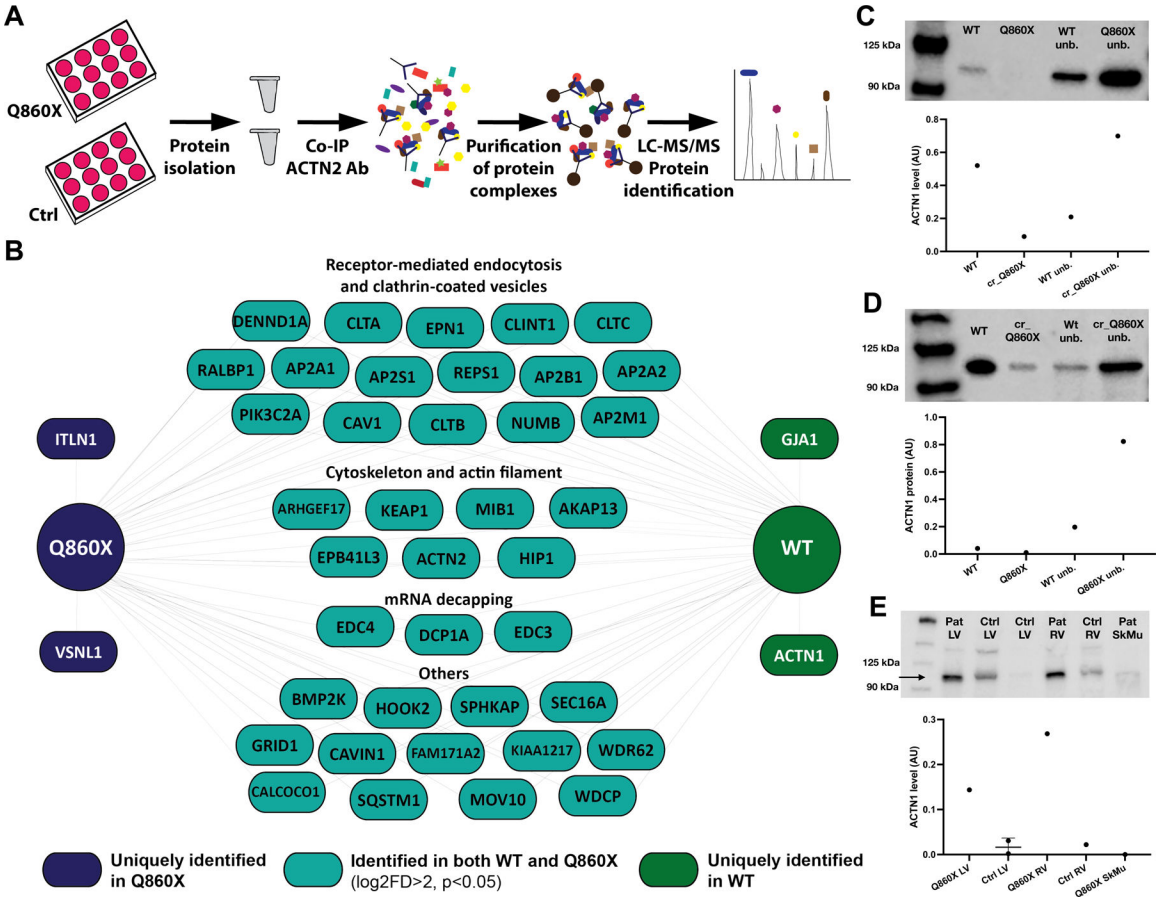


**Fig. 4. The cardiomyocyte ACTN2 interactome identifies C-terminal region to be necessary for interaction with ACTN1.**

A) Experimental set-up of the co-immunoprecipitation followed by mass-spectrometry. IgG pulldown was used as a negative control. B) Mass-spectrometry analysis identified a common ACTN2 interactome in all hiPSC-CMs in turquoise (iLogFD>2, iPvalue<0.05 in both conditions, at least 3 peptides used for analysis, see Supplemental methods and Dataset IX for details). Proteins significantly different between conditions and identified only in the WT (n=3) are shown in dark green and proteins uniquely identified in Q860X (n=3) in dark blue. C) Co-immunoprecipitation of ACTN2 followed by Western blot using an ACTN1 antibody showed interaction only in WT cells compared to Q860X, in concordance with the Co-IP mass-spec data. D) Co-immunoprecipitation of ACTN2 followed by Western blot using an ACTN1 antibody showed interaction only in WT cells compared to cr_Q860X. E) Expression of ACTN1 in Q860X explanted cardiac LV and RV compared to healthy control individuals. Dot plots show individual quantifications from Western Blot. The control LV in panel E shows the mean ± SEM for the two control individuals.